Acta Cryst. (1990). B46, 166–174

Electron-Density Distribution in Crystals of $K_2[MCl_6]$ (M = Re, Os, Pt) and $K_2[PtCl_4]$ at 120 K

BY HIROYUKI TAKAZAWA, SHIGERU OHBA AND YOSHIHIKO SAITO*

Department of Chemistry, Faculty of Science and Technology, Keio University, Hiyoshi 3, *Kohoku-ku, Yokohama* 223, *Japan*

AND MITSURU SANO

Department of Chemistry, College of General Education, Nagoya University, Chikusa-ku, Nagoya 464-01, *Japan*

(*Received* 25 *August* 1989; *accepted* 13 *November* 1989)

Abstract

T = 120 (2) K. Dipotassium hexachlororhenate(IV), $K_2[ReCl_6]$, (I): M_r = 477·1, cubic, $Fm3m$, Z = 4, a = 9·7953 (5) Å, V = 939·84 (14) Å^3, D_x = 3·37 Mg m^{-3}, Ag $K\alpha$, λ = 0·56083 Å, μ = 8·26 mm^{-1}, $F(000)$ = 859·1, final R = 0·0219 for 346 unique reflections. Dipotassium hexachloroosmate(IV), $K_2[OsCl_6]$, (II): M_r = 481·1, cubic, $Fm3m$, Z = 4, a = 9·7195 (8) Å, V = 918·19 (21) Å^3, D_x = 3·48 Mg m^{-3}, μ(Ag $K\alpha$) = 8·81 mm^{-1}, $F(000)$ = 862·8, final R = 0·0194 for 244 unique reflections. Dipotassium hexachloroplatinate(IV), $K_2[PtCl_6]$, M_r = 486·0, cubic, $Fm3m$, Z = 4; (III*a*) Ag $K\alpha$: a = 9·6911 (7) Å, V = 910·16 (21) Å^3, D_x = 3·55 Mg m^{-3}, μ = 9·70 mm^{-1}, $F(000)$ = 870·1, final R = 0·0159 for 343 unique reflections; (III*b*) Mo $K\alpha_1$: a = 9·6862 (3) Å, V = 908·78 (4) Å^3, D_x = 3·55 Mg m^{-3}, μ = 18·22 mm^{-1}, $F(000)$ = 868·1, final R = 0·0113 for 403 unique reflections. Dipotassium tetrachloroplatinate(II), $K_2[PtCl_4]$, M_r = 415·1, tetragonal, $P4/mmm$, Z = 1; (IV*a*) Ag $K\alpha$: a = 6·9961 (8), c = 4·1051 (8) Å, V = 200·93 (6) Å^3, D_x = 3·43 Mg m^{-3}, μ = 10·64 mm^{-1}, $F(000)$ = 183·4, final R = 0·0194 for 683 unique reflections; (IV*b*) Mo $K\alpha_1$: a = 6·9813 (3), c = 4·1048 (3) Å, V = 200·06 (2) Å^3, D_x = 3·45 Mg m^{-3}, μ = 20·01 mm^{-1}, $F(000)$ = 182·8, final R = 0·0147 for 942 unique reflections. The charge asphericity caused by the 5*d* electrons could be clearly observed in the octahedral and square-planar chloro complexes by the X-ray diffraction method using Ag $K\alpha$ radiation at 120 K. Because of sharp deformation density located outside the high-density inner core region, even the *d* electrons in 5*d* orbitals could be detected in spite of very small valence/total electron ratios. In the octahedral complexes (I)–(III), positive deformation densities corresponding to t_{2g} (d_{xy}, d_{xz}, d_{yz}) orbitals were observed in the [111] directions. Above and below the coordination plane of $[PtCl_4]^{2-}$, excess densities were recognized, suggesting an excess a_{1g} (d_{z^2}) orbital population. These charge asphericities could be reproduced by the multipole expansion method with reasonable *d*-orbital populations, and could not be deleted by anharmonic thermal-vibration analysis. Theoretical deformation densities of $[PtCl_6]^{2-}$ and $[PdCl_6]^{2-}$ calculated by the *DV-Xα* MO self-consistent-charge method indicated that the sharp deformation density of the *d* electrons is the result of contraction of valence orbitals in the ligand field.

Introduction

As an extension of our systematic studies on transition-metal complexes (Takazawa, Ohba & Saito, 1988; and references therein), we have investigated 5*d* transitional-metal complexes. It may be more difficult to detect the charge asphericity of the 4*f* or 5*d* electrons than that of 3*d* electrons, because of the relatively small contribution to diffracted intensities (Stevens & Coppens, 1976). Furthermore, serious experimental error may be caused by a failure of the absorption correction. Chatterjee, Maslen & Watson (1989) reported the 4*f* electron distributions in a series of lanthanoid complexes $[Ln(H_2O)_6](CF_3SO_3)_3$ (Ln = La, Ce, Pr, Nd, Sm, Eu, Gd, Tb, Dy, Yb and Lu).

The aim of our study is to detect aspherical 5*d*-electron distribution beyond the experimental errors. This will be on a borderline of the experimental technique, inside the safety region of which lie the studies on 3*d* and 4*d* transition-metal complexes. In order to reduce the ambiguity caused by structural parameters, crystals with high symmetry such as $K_2[PtCl_6]$ and $K_2[PtCl_4]$ were selected and experimental resolution was improved by lowering the temperature. Both Ag $K\alpha$ and Mo $K\alpha$ radiations were used to see the effect of absorption error. The

* To whom correspondence should be addressed.

0108-7681/90/020166-09$03.00

© 1990 International Union of Crystallography

compounds of Re, Os and Ir having the $K_2[PtCl_6]$ structure were also investigated to show the reliability of the present study. Preliminary studies of $K_2[PtCl_4]$ (Ohba, Sato, Saito, Ohshima & Harada, 1983) and $K_2[PtCl_6]$ (Ohba & Saito, 1984) at room temperature have been reported previously. Isomorphous 4*d* metal complexes, $K_2[PdCl_6]$ and $K_2[PdCl_4]$, have already been examined at 120 K as a first step in the present study (Takazawa, Ohba & Saito, 1988).

Experimental

Preparation of crystals

(I): 7 ml of 35% aqueous HCl was poured onto a mixture of 2 g of KI and 1 g of $KReO_4$ in an evaporating dish, and warmed on a water bath at 363 K for 1 h. During warming 5 ml of 35% aqueous HCl was gradually added. After evaporation was completed, 10 ml of hot 10% aqueous HCl was poured onto the residue and the solution filtered. Crude crystals were obtained by cooling the filtrate in an ice bath. Light-green octahedra surrounded by {111} faces were grown from a concentrated HCl solution.

(II): 1 g of Os_2O_7, 10 g of $FeCl_2.nH_2O$ and 30 ml of 35% aqueous HCl were mixed in a flask with a cork stopper. After warming at 373 K for 2 h, 10 ml of 1*M* KCl solution was added and the resulting solution cooled in an ice bath for 1 h. Crude crystals were separated by a glass filter and washed with absolute ethanol. Dark-red octahedra with {111} forms were grown from a hot aqueous solution containing a small amount of HCl.

(III) and (IV): By recrystallization from an aqueous solution of the commercial products, orange octahedra with {111} forms and ruby-red prisms elongated along *c* were obtained, respectively.

$K_2[IrCl_6]$ crystals were obtained by slow cooling of a mixture of $IrCl_4$ and KCl solutions; however, they were unsuitable for X-ray diffraction studies.

Data collection

Specimens were shaped into spheres (Bond, 1951). They were cooled in a stream of cold nitrogen gas with the temperature maintained at 120 (2) K. Intensities were measured on a Rigaku AFC-5 automated four-circle diffractometer with a detector aperture of $1{\cdot}55 \times 1{\cdot}55°$; θ–2θ scan technique with a scan speed of $6° \text{ min}^{-1}$ in θ. Lattice constants were based on 10 2θ values ($20 < 2\theta < 30°$) for (I)–(III*a*), 16 2θ values ($20 < 2\theta < 30°$) for (IV*a*), and 20 2θ values ($60 < 2\theta < 70°$) for (III*b*) and (IV*b*). The polarization factor of the monochromator was assumed to be $(1 + \cos 2\theta_M)/2$ (Jennings, 1984). The experimental conditions are listed in Table 1.

Refinement

Conventional refinement

Conventional refinement (refinement *A*) was performed with the full-matrix least-squares program *RADIEL* (Coppens, Guru Row, Leung, Stevens, Becker & Yang, 1979) although parameters for atomic charges and κ parameters were not refined, corresponding to the program *LINEX* (Becker & Coppens, 1975). The function $\sum w(|F_o| - |F_c|)^2$ was minimized with weight $w^{-1} = \sigma^2(|F_o|) + (0{\cdot}015|F_o|)^2$. Complex neutral-atom scattering factors were taken from *International Tables for X-ray Crystallography* (1974). Positional and thermal parameters were determined based on all the observed unique reflections because bias by the valence electrons could be neglected for heavy atoms (Takazawa, Ohba & Saito, 1988). When an isotropic secondary-extinction parameter of type I (Becker & Coppens, 1975) was introduced, *R* values for all the observed unique reflections reduced as follows: (I) 0·0283→0·0219, (II) 0·0196→0·0194, (III*a*) 0·0253→0·0159, (III*b*) 0·0248→0·0113, (IV*a*) 0·0329→0·0194 and (IV*b*) 0·0200→0·0147.* The smallest value of F_o^2/F_c^2 was in the range 0·55–0·77. Reflection/parameter ratios were (I) 49·4, (II) 34·9, (III*a*) 49·0, (III*b*) 57·6, (IV*a*) 62·1 and (IV*b*) 85·6. Other refinement information is listed in Table 2. Calculations were carried out on a FACOM M-380R computer of Keio University.

Multipole expansion

Multipole refinement was performed with the program *MOLLY* (Hansen & Coppens, 1978). Multipoles were introduced up to the hexadecapole level for Re, Os, Pt and Cl atoms. The radial functions were $r^{n_l}\exp(-\zeta r)$ with $n_l = 4$ for all the *l* values. An isotropic secondary-extinction parameter of type I with Lorentzian distribution (Becker & Coppens, 1975) was introduced. The core and valence scattering factors for Re, Os and Pt were obtained from a Fourier transform of the wavefunctions tabulated by Mann (1967). The core and valence scattering factors for the Cl atom and the scattering factor of the K^+ ion were taken from *International Tables for X-ray Crystallography* (1974). The core electron configurations were assumed to be Xe core + $(4f)^{14}$ for

* Lists of structure factors based on refinement *A* for (I) and (II) and those based on refinement *C* for others, refinement information for multipole and anharmonic vibration analyses, multipole parameters, model deformation densities based on refinement *C*, and residual densities for (IV) and $K_2[PdCl_4]$ based on refinements *D* and *E* have been deposited with the British Library Document Supply Centre as Supplementary Publication No. SUP 52462 (46 pp.). Copies may be obtained through The Technical Editor, International Union of Crystallography, 5 Abbey Square, Chester CH1 2HU, England.

Table 1. *Experimental conditions*

	(I)	(II)	(III*a*)	(III*b*)	(IV*a*)	(IV*b*)
Diameter of specimen, $2r$ (mm)	0·261 (6)	0·287 (5)	0·237 (6)	0·209 (6)	0·233 (6)	0·40 (1)
Radiation	Ag $K\alpha$	Ag $K\alpha$	Ag $K\alpha$	Mo $K\alpha$	Ag $K\alpha$	Mo $K\alpha$
Wavelength (Å)	0·56083	0·56083	0·56083	0·70926	0·56083	0·70926
Monchromator	LiF	LiF	LiF	Graphite	LiF	Graphite
Diameter of collimator, Ø (mm)	0·7	0·7	0·7	0·5	0·7	1·0
A and B in scan width $(A + B\tan\theta)^\circ$	1·3, 0·36	1·4, 0·36	1·3, 0·36	1·3, 0·36	1·3, 0·36	1·4, 0·5
Variation of standards	0·99–1·00	0·98–1·00	0·95–1·00	0·99–1·00	0·98–1·00	0·99–1·01
Range of indices	(*a*)	(*a*)	(*a*)	(*b*)	(*c*)	(*d*)
No. of measured reflections	2923	2911	2897	5109	3087	4712
No. of observed reflections with $\lvert F_o\rvert > 3\sigma(\lvert F_o\rvert)$	2665	2201	2670	5109	2958	4711
No. of unique reflections	346	244	343	403	683	942
Internal agreement, R_{int}	0·024	0·024	0·019	0·022	0·023	0·025
Linear absorption coefficient, μ (mm^{-1})	8·26	8·81	9·70	18·22	10·64	20·01
μr	1·08	1·26	1·15	1·90	1·24	4·00
Transmission factors	0·219–0·256	0·172–0·211	0·200–0·245	0·080–0·160	0·178–0·218	0·012–0·069

Notes: (*a*) $-14 \le h, k \le 14, 0 \le l \le 14$ ($0 < 2\theta \le 50°$), $0 \le h, k, l \le 22$ ($50 < 2\theta \le 80°$); (*b*) $-17 \le h, k \le 17, 0 \le l \le 17$ ($0 < 2\theta \le 80°$), $0 \le h, k, l \le 23$ ($80 < 2\theta \le 120°$); (*c*) $-10 \le h, k \le 10, 0 \le l \le 6$ ($0 < 2\theta \le 50°$), $-16 \le h \le 16, 0 \le k \le 16, 0 \le l \le 9$ ($50 < 2\theta \le 80°$); (*d*) $-12 \le h, k \le 12, 0 \le l \le 6$ ($0 < 2\theta \le 80°$), $-17 \le h \le 17, 0 \le k \le 17, 0 \le l \le 10$ ($80 < 2\theta \le 120°$).

Table 2. *Refinement information for conventional refinement (refinement A)*

	(I)	(II)	(III*a*)	(III*b*)	(IV*a*)	(IV*b*)
R	0·0219	0·0194	0·0159	0·0113	0·0194	0·0147
wR	0·0275	0·0223	0·0210	0·0152	0·0214	0·0203
S	1·27	0·99	0·98	0·84	0·93	1·02
g ($\times 10^{-4}$)	0·104 (12)	0·072 (8)	0·153 (11)	0·232 (10)	0·262 (10)	0·089 (5)
Min. of y (F_o^2/F_c^2)	0·72	0·77	0·66	0·55	0·56	0·71
$(\Delta/\sigma)_{max}$	0·001	0·003	0·03	0·01	0·02	0·01
M—Cl distance (Å)	2·3545 (9)	2·3337 (9)	2·3164 (8)	2·3152 (5)	2·3119 (4)	2·3080 (2)

Re, Os and Pt atoms; and Ne core for the Cl atom. Refinements were performed without taking the 6*s* and 6*p* density functions into consideration, because Holladay, Leung & Coppens (1983) showed that the 3*d* electron populations were almost independent of the treatment of the 4*s* electron. The 6*s* and 6*p* electron distributions are more diffuse than 4*s*, thus they were neglected in the refinements. The neutral charge of crystals was constrained with the charge for K^+ fixed at +1. The positional, thermal and multipole parameters were refined. The ζ values were fixed to be 4·0 a.u.$^{-1}$ for Re, Os and Pt (Eyring, Walter & Kimball, 1944) and 4·0 a.u.$^{-1}$ for Cl (Clementi & Raimondi, 1963). The radial parameter, κ (Coppens, Guru Row, Leung, Stevens, Becker & Yang, 1979), for Cl was fixed at 1·0. All the observed unique reflections were used for the refinements. Since the effective charge of the central metal atoms of (I) and (II) converged to unreasonable negative values, the refinements were continued only for (III) and (IV). For (III), the Pt and Cl atoms lie on special positions with site symmetry, *m*3*m* and 4*mm*, respectively, the number of multipole parameters being 2 and 6, respectively. The local axes of the multipole functions for the Pt atom were taken along the crystal axes, *i.e.* the Pt—Cl bond directions. The number of electrons of the t_{2g} (d_{xy}, d_{xz}, d_{yz}) orbitals was fixed at 6 to keep Pauli's exclusion principle since the number became much greater than 6 when multipoles were refined without the constraint. For (IV), the Pt and Cl atoms lie on special positions with site symmetry, 4/*mmm* and *mm*2, respectively, and the number of multipole parameters is 4 and 9, respectively. The local x and y axes of the multipole functions for the Pt atom were taken along the Pt—Cl bond directions and the z axis along the fourfold axis. The number of electrons of the a_{1g} (d_{z^2}), e_g (d_{xz}, d_{yz}) and b_{2g} (d_{xy}) orbitals converged to values greater than 2, 4 and 2, respectively; thus they were fixed at 2, 4 and 2, respectively. The model deformation densities, ρ_{model} ($= \rho_{calc,multipole} - \rho_{calc,spherical}$) after refinement with the κ value fixed at unity (refinement *B*) did not reproduce the feature of aspherical distribution around the Pt atom. Consequently, the κ parameter of Pt was refined (refinement *C*) and the reproduction of asphericity was achieved successfully. The introduction of multipoles did not improve the R values except for (III*b*): (III*a*) 0·0166→0·0164, (III*b*) 0·0117→0·0102, (IV*a*) 0·0198→0·0197 and (IV*b*) 0·0148→0·0148.* This is because of the relatively small contribution of valence electrons in the X-ray diffraction intensities for these heavy-metal complexes.

Anharmonic thermal-vibration analysis

The observed features of the deformation density around the metal atom seem to be due to 5*d* electrons and not due to anharmonic thermal vibrations. In order to confirm this observation, a temporary refinement was carried out for platinum complexes with the program *LINKT* (Tanaka & Marumo, 1983; refinement *D*). Anharmonic thermal-vibration

* See deposition footnote.

Table 3. *Positional* ($\times 10^5$) *and thermal* ($\times 10^5$ Å^2) *parameters*

The thermal parameters are expressed as follows: $\exp[-2\pi^2(h^2a^{*2}U_{11} + k^2b^{*2}U_{22} + l^2c^{*2}U_{33} + 2hka^*b^*U_{12})]$. First row: conventional refinement; second row: multipole refinement (refinement *C*).

	x	*y*	*z*	U_{11} or U_{iso}	U_{22}	U_{33}	U_{12}
(I)							
Re	0	0	0	646 (8)			
Cl	24037 (9)	0	0	767 (27)	2155 (28)	(= U_{22})	
K	25000	25000	25000	2240 (32)			
(II)							
Os	0	0	0	576 (8)			
Cl	24011 (9)	0	0	619 (23)	2032 (24)	(= U_{22})	
K	25000	25000	25000	1627 (22)			
(III*a*)							
Pt	0	0	0	561 (5)			
	0	0	0	542 (6)			
Cl	23902 (8)	0	0	710 (21)	1969 (20)	(= U_{22})	
	23893 (9)	0	0	710 (28)	1977 (23)	(= U_{22})	
K	25000	25000	25000	1645 (19)			
	25000	25000	25000	1649 (19)			
(III*b*)							
Pt	0	0	0	662 (3)			
	0	0	0	641 (3)			
Cl	23902 (4)	0	0	808 (11)	2116 (12)	(= U_{22})	
	23902 (5)	0	0	806 (14)	2114 (12)	(= U_{22})	
K	25000	25000	25000	1778 (11)			
	25000	25000	25000	1777 (11)			
(IV*a*)							
Pt	0	0	0	703 (5)	(= U_{11})	935 (7)	
	0	0	0	662 (7)	(= U_{11})	893 (8)	
Cl	23367 (6)	(= *x*)	0	980 (12)	(= U_{11})	1869 (24)	− 125 (15)
	23375 (8)	(= *x*)	0	995 (15)	(= U_{11})	1875 (31)	− 112 (20)
K	0	50000	50000	2243 (36)	1312 (28)	1181 (26)	
	0	50000	50000	2255 (35)	1325 (27)	1193 (26)	
(IV*b*)							
Pt	0	0	0	694 (3)	(= U_{11})	947 (4)	
	0	0	0	637 (3)	(= U_{11})	925 (4)	
Cl	23377 (4)	(= *x*)	0	975 (7)	(= U_{11})	1847 (16)	− 111 (9)
	23380 (5)	(= *x*)	0	987 (8)	(= U_{11})	1873 (19)	− 109 (10)
K	0	50000	50000	2236 (24)	1265 (17)	1134 (16)	
	0	50000	50000	2259 (23)	1281 (16)	1149 (16)	

parameters were introduced for Pt instead of multipole parameters. Isotropic secondary extinction was corrected by assuming Lorentzian type-I distribution (Becker & Coppens, 1975). Complex neutral-atom scattering factors were taken from *International Tables for X-ray Crystallography* (1974). Positional and harmonic themal parameters were fixed at the values of the conventional refinement (refinement *A*) to prevent divergence. $K_2[PdCl_6]$ and $K_2[PdCl_4]$ data were also tested (Takazawa, Ohba & Saito, 1988). For $K_2[PtCl_6]$ (III) and $K_2[PdCl_6]$, the number of anharmonic parameters for the Pt and Pd atoms is 2. The local coordinates were taken as in the multipole refinements. *R* factors did not alter for (III*a*) 0·0159 and (III*b*) 0·0114, except for $K_2[PdCl_6]$ 0·0132→0·0125. For $K_2[PtCl_4]$ (IV) and $K_2[PdCl_4]$, the number of anharmonic parameters for the central metal atoms is 4. *R* factors were not significantly improved: (IV*a*) 0·0194→0·0192, (IV*b*) 0·0147→0·0146 and $K_2[PdCl_4]$ 0·0209→0·0211.

The charge asphericity and the effect of the anharmonic thermal vibration seem to differ in the $(\sin\theta)/\lambda$ dependence. The contribution of the valence density to the scattering factor decreases in the high-angle region; however, the effect of anharmonic vibration rapidly increases (Ohba, Saito & Wakoh, 1982). To explore this point, a temporary refinement was also carried out excluding high-order reflections with $[(\sin\theta)/\lambda]_{max} = 1{\cdot}0$ Å^{-1} (refinement *E*). The *R* values for the reflections with $(\sin\theta)/\lambda \leq 1{\cdot}0$ Å^{-1} reduced: (III*b*) 0·0107→0·0103 and $K_2[PdCl_6]$ 0·0121→0·0106, whereas those for all the reflections increased: (III*b*) 0·0114→0·0117 and $K_2[PdCl_6]$ 0·0125→0·0134. The result indicated the importance of high-order reflections for distinguishing charge asphericity from anharmonic vibration as will be discussed later in *Results and discussion*.

Theoretical calculations

The electron-density distribution in the $[PdCl_6]^{2-}$ and $[PtCl_6]^{2-}$ complex anions has been investigated by one of the authors (MS) by means of the *DV-Xα* MO self-consistent-charge (SCC) method. The computational details of the *DV-Xα* MO SCC method have been thoroughly described by Adachi, Tsukada & Satoko (1978). In the Hartree–Fock–

Slater method, the exchange-correlation term is given by

$$-3\alpha\{[3/(8\pi)]\rho(r)\}^{1/3}$$

where $\rho(r)$ is the local charge density and α is the exchange-scaling parameter; the value of $\alpha = 0.7$ was used for all atoms throughout the present calculations. Basis sets including the Pt 1*s*–6*p*, Pd 1*s*–5*p*, Cl 1*s*–3*d* orbitals were utilized for the present calculations. The molecular geometries of the complexes were taken from the experimental results.

Results and discussion

Conventional deformation density

Atomic parameters are given in Table 3. The metal—Cl distances are listed in Table 2. Deformation densities were calculated based on the observed unique reflections with $(\sin\theta)/\lambda \le 1.00$ Å^{-1}, except for (II) [$(\sin\theta)/\lambda \le 0.85$ Å^{-1}], to reduce the noise level of the maps. Anomalous scattering was corrected after Ibers & Hamilton (1964). An alternative correction for anomalous scattering gave no significant variation of the deformation density (Takazawa, Ohba & Saito, 1988). Sections of the (110) plane for the $K_2[MCl_6]$ (M = Re, Os, Pt) crystals are shown in Fig. 1. The positive peaks on the threefold axes and negative troughs on the metal—Cl bond axes indicate an excess 5*d* electron population in the t_{2g} orbitals and a deficiency in the e_g orbitals of the metal atom. The peak heights and the distances from the metal nucleus are listed in Table 4. The similar charge asphericities around the Pt nucleus in $K_2[PtCl_6]$ were detected by using Ag $K\alpha$ (III*a*) and Mo $K\alpha$ (III*b*) data in a qualitative

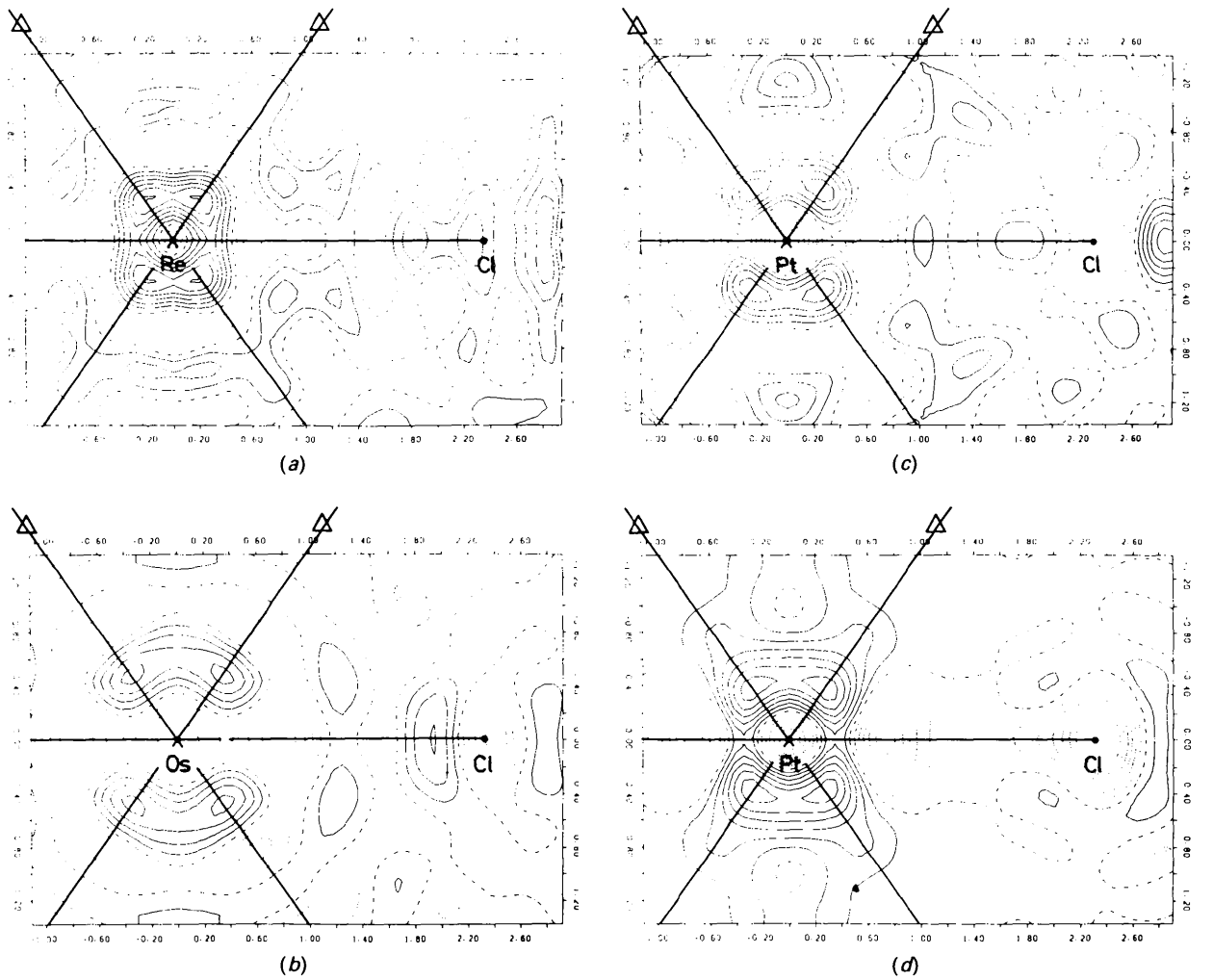

Fig. 1. Deformation densities on the (110) plane of (*a*) $K_2[ReCl_6]$, (*b*) $K_2[OsCl_6]$, (*c*) $K_2[PtCl_6]$ (Ag $K\alpha$ data) and (*d*) $K_2[PtCl_6]$ (Mo $K\alpha$ data). The cut-off value, $[(\sin\theta)/\lambda]_{max}$, is 1.0 Å^{-1} except for $K_2[OsCl_6]$, 0.85 Å^{-1}. Contour intervals at 0.2 e Å^{-3}. Negative contours broken, zero contours chain-dotted.

sense. The data indicate that meaningful results were obtained in spite of the heavy absorption effect. Sections of the (100) and (001) planes for the $K_2[PtCl_4]$ crystals are shown in Fig. 2. A positive peak is located above and below the Pt nucleus at 0·5 Å from the $[PtCl_4]^{2-}$ plane. In the plane of the complex anion, the deformation density is higher in the direction of the bisector of the Cl—Pt—Cl bond angle than that on the Pt—Cl bond axis. These observations indicate the excess $5d$ electron population in the a_{1g} (d_{z^2}) and b_{2g} (d_{xy}) orbitals and a population deficiency in the b_{1g} ($d_{x^2-y^2}$) orbital.

Theoretical static deformation densities in the (110) plane of $[PdCl_6]^{2-}$ and $[PtCl_6]^{2-}$ anions calculated with the *DV-Xα* MO SCC method show almost the same aspherical *d*-electron distribution (Fig. 3), where the reference density is the superposition of the spherically averaged densities of neutral atoms. The observed excess electron density on the threefold axis was supported by the theory. Although the metal atoms have positive effective charge, they are surrounded with positive deformation densities. This is due to the contraction of the valence orbitals of the metal atom in the ligand field, and is the reason why the broadly distributed *d* electrons in the atom can be detected as a sharp deformation density in the complex.

Multipole expansion

The wavefunctions tabulated by Mann (1967) did not involve the relativistic effect. However, the effect might be approximately corrected by small thermal parameters. When the conventional refinement was performed for (III) and (IV) by using the scattering factors of Pt transformed from Mann's wavefunctions instead of those listed in *International Tables for X-ray Crystallography* (1974) including the rela-

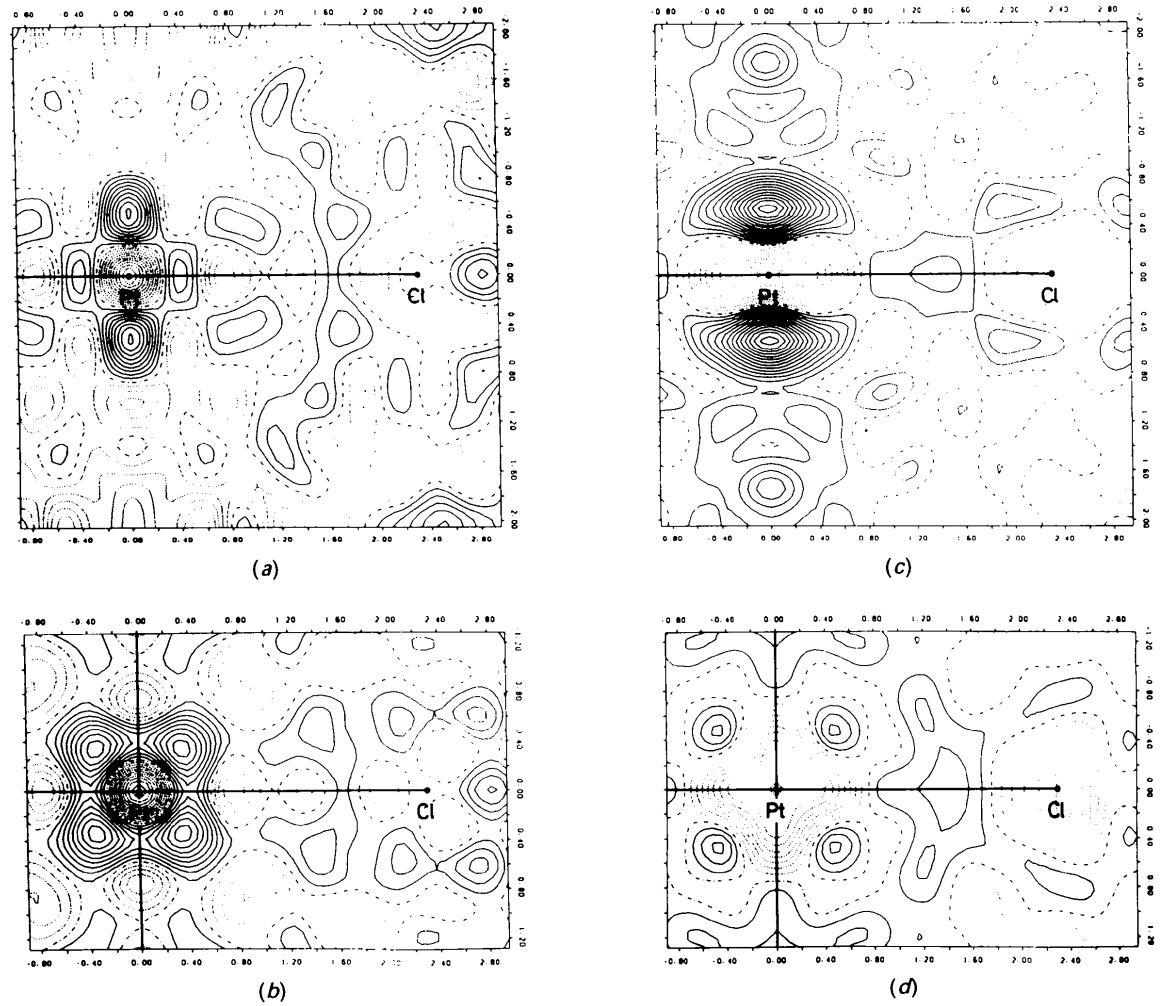

Fig. 2. Deformation densities on (*a*) the (100) and (*b*) (001) planes of $K_2[PtCl_4]$ (Ag $K\alpha$ data), and (*c*) the (100) and (*d*) (001) planes of $K_2[PtCl_4]$ (Mo $K\alpha$ data). $[(\sin\theta)/\lambda]_{max} = 1{\cdot}0$ Å^{-1}, contour intervals at 0·2 e Å^{-3}.

Table 4. *Peak heights* (e Å^{-3}) *and their distances from the central metal atom* (Å)

(i) On the threefold axes for $K_2[MCl_6]$ (M = Re, Os and Pt)

	Height	Distance
(I)	+ 1·2 (3)	0·38
(II)	+ 0·8 (2)	0·58
(III*a*)	+ 0·9 (3)	0·46
(III*b*)	+ 1·3 (3)	0·47

(ii) On the fourfold axes for $K_2[PtCl_4]$

	Height	Distance
(IV*a*)	+ 1·8 (4)	0·52
(IV*b*)	+ 2·8 (3)	0·47

(iii) On the direction bisecting the Cl—Pt—Cl angle for $K_2[PtCl_4]$

	Height	Distance
(IV*a*)	+ 1·6 (4)	0·50
(IV*b*)	+ 0·7 (3)	0·54

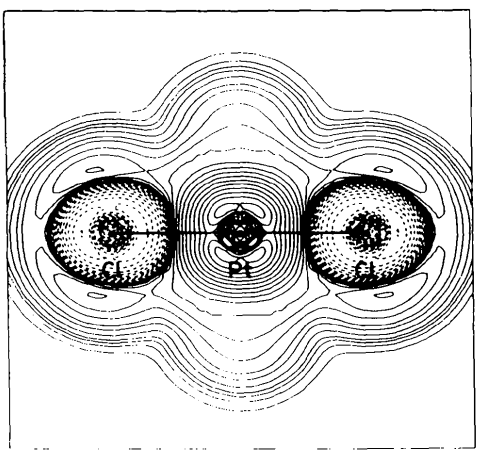

(*a*)

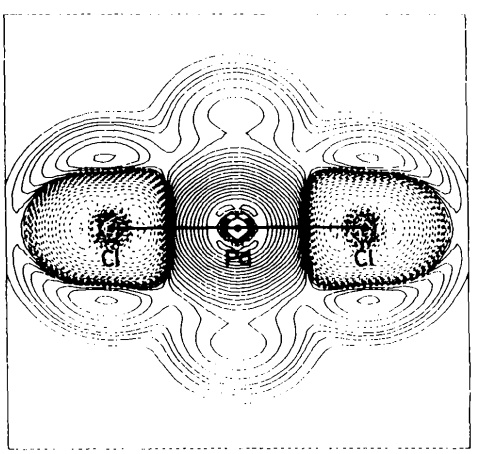

(*b*)

Fig. 3. Section of the theoretical static deformation densities through two threefold axes and a metal—Cl bond axis for (*a*) $[PtCl_6]^{2-}$ and (*b*) $[PdCl_6]^{2}$ complex anions. The contours are from ±2·2 to ±0·0007 e Å^{-3}. Neighbouring contours differ by a factor of $\sqrt{2}$.

tivistic effect, R values did not change within 0·07% and deformation densities did not alter significantly.

The model deformation maps, $\Delta\rho_{\text{model}}$ ($= \rho_{\text{calc,multipole}} - \rho_{\text{calc,spherical}}$), based on refinement C reproduce the aspherical distribution of 5*d* electrons,* whereas those based on refinement B do not because the κ parameter was fixed at unity in this refinement. All the refined κ values from refinement C are greater than unity [1·03 (4)–1·21 (3)], suggesting contraction of valence density of the metal atoms in agreement with the theoretical prediction (Fig. 3).

The *d*-electron populations listed in Table 5 were derived from the multipole coefficients (Takazawa, Ohba & Saito, 1988). Since both (III) and (IV) are in low-spin states, the t_{2g} orbitals of (III) and the b_{2g}, e_g and a_{1g} orbitals of (IV) are fully occupied in the ligand-field approximation with d^6 and d^8 configurations, respectively. The populations of e_g orbitals in (III) and b_{1g} orbitals in (IV) suggest that the Pt atoms are neutralized by the coordinated Cl^- ions.

Effective charges of the central metal atoms were also estimated by direct integration of the electron densities. The number of electrons in a sphere centered on the metal atoms was calculated where the series-termination correction was taken into account. The effective radii of the Re, Os and Pt atoms were estimated to be 1·2 Å, from a minimum of the radical distribution curves. The effective charges measured by ESCA and NQR are also listed in Table 6. Although the definitions of the effective charge differ from each other, these results suggest that the central metal atoms are largely neutralized from the formal positive charge.

Anharmonic thermal-vibration analysis

The residual densities, $\Delta\rho_{\text{residual}}$ ($= \rho_{\text{obs}} - \rho_{\text{calc,anharm}}$), based on refinement D, in which anharmonic thermal parameters were introduced without multipole parameters, are shown in Fig. 4 for $K_2[PtCl_6]$ and $K_2[PdCl_6]$. In these maps, the characteristic features around the central metal atom almost totally remain, clearly indicating that the observed features are not due to anharmonic thermal vibration. Furthermore, the corresponding δ value became negative for $K_2[PtCl_6]$, (III*a*) $-1{\cdot}6\,(5) \times 10^{-18}$ and (III*b*) $-0{\cdot}22\,(9) \times 10^{-18}$ J Å^{-4}, although δ is expected to be positive for an octahedral complex (Willis, 1969). The inconsistent δ values also imply that anharmonic thermal-vibration analysis was inappropriate for the present case.

Mallinson, Koritsanszky, Elkaim, Li & Coppens (1988) made a temporary analysis of anharmonic thermal vibration for the static $[Fe(H_2O)_6]^{3+}$ ion based on the theoretical structure factors up to $(\sin\theta)/\lambda = 1{\cdot}2$ Å^{-1} and showed that the charge

* See deposition footnote.

Table 5. *Electron populations in each d orbital*

	(III*a*)		(III*b*)		$K_2[PdCl_6]$*
Refinement	*B*	*C*	*B*	*C*	
κ	1·0	1·03 (4)	1·0	1·12 (3)	1·09 (2)
e_g ($d_{x^2-y^2}$, d_{z^2})	3·23 (13)	2·97 (15)	2·82 (12)	2·12 (12)	1·89 (7)
t_{2g} (d_{xy}, d_{xz}, d_{yz})	6·0†	6·0†	6·0†	6·0†	6·14 (8)
Total	9·23 (13)	8·97 (15)	8·82 (12)	8·12 (12)	8·03 (10)
Effective charge	+ 0·77 (13)	+ 1·03 (15)	+ 1·18 (12)	+ 1·88 (12)	+ 1·97 (10)
	(IV*a*)		(IV*b*)		$K_2[PdCl_4]$*
Refinement	*B*	*C*	*B*	*C*	
κ	1·0	1·21 (3)	1·0	1·08 (2)	1·12 (1)
b_{1g} ($d_{x^2-y^2}$)	1·24 (6)	0·33 (6)	0·70 (6)	0·33 (6)	1·49 (3)
b_{2g} (d_{xy})	2·0†	2·0†	2·0†	2·0†	2·0†
e_g (d_{xz}, d_{yz})	4·0†	4·0†	4·0†	4·0†	4·0†
a_{1g} (d_{z^2})	2·0†	2·0†	2·0†	2·0†	2·0†
Total	9·24 (6)	8·33 (6)	8·70 (6)	8·33 (6)	9·49 (3)
Effective charge	+ 0·76 (6)	+ 1·67 (6)	+ 1·30 (6)	+ 1·67 (6)	+ 0·51 (3)

* Takazawa, Ohba & Saito (1988).
† These values were fixed (see text).

Table 6. *Effective charge of the central metal atoms*

	Formal	MR[a]		DI[b]	ESCA	NQR	
(I)	+ 4			+ 1·6 (3)	+ 1·6 (1)[c]	+ 0·70[d]	+ 1·34[e]
(II)	+ 4			+ 2·5 (3)	+ 1·6 (1)[c]	+ 0·80[f]	+ 1·06[e]
(III*a*)	+ 4	+ 0·77 (13)[g]	+ 1·03 (15)[h]	+ 1·6 (3)	+ 1·3 (1)[c]	+ 0·64[i]	+ 0·70[e]
(III*b*)	+ 4	+ 1·18 (12)[g]	+ 1·88 (12)[h]	+ 1·3 (8)			
$K_2[PdCl_6]$	+ 4		+ 1·97 (10)[j]	+ 1·2 (4)[j]	+ 1·4 (1)[c]	+ 0·58[k]	
(IV*a*)	+ 2	+ 0·76 (6)[g]	+ 1·67 (6)[h]	+ 1·0 (3)	+ 0·4 (2)[l]	+ 0·4[m]	
(IV*b*)	+ 2	+ 1·30 (6)[g]	+ 1·67 (6)[h]	+ 0·3 (5)			
$K_2[PdCl_4]$	+ 2		+ 0·51 (3)[j]	+ 0·6 (4)[j]	+ 0·4 (2)[l]		

Notes: (*a*) multipole refinement; (*b*) direct integration; (*c*) Larsson & Forkesson (1977): $(Ph_4P)_2[MCl_6]$ (M = Pt, Pd); (*d*) Ikeda, Nakamura & Kubo (1965); (*e*) Brown, McDugle & Kent (1970); (*f*) Ito, Nakamura, Kurita, Ito & Kubo (1961); (*g*) refinement *B*; (*h*) refinement *C*; (*i*) Nakamura, Kurita, Ito & Kubo (1960); (*j*) Takazawa, Ohba & Saito (1988); (*k*) Ito, Nakamura, Kurita, Ito & Kubo (1963); (*l*) Forkesson & Larsson (1976): $(Ph_4P)_2[MCl_4]$ (M = Pt, Pd); (*m*) Marram, McNiff & Ragle (1963).

asphericity of the 3*d* electrons could be completely deleted by the Gram–Charlier formalism. In this case, the $[(\sin\theta)/\lambda]_{max}$ limit might be too low to distinguish the *d* electron asphericity from the anharmonic vibrations. The localized charge density has significant scattering power even in the high-order region as seen from the series-termination effect on the deformation density of the 3*d* electrons (Ohba, Toriumi, Sato & Saito, 1978). The theoretical trial may yield different results if the thermal smearing of the charge density is taken into account. In the present study charge asphericity could be distinguished from the anharmonic thermal vibration. To show the important role of high-order reflections, an inadvisable refinement was carried out purposely. Fig. 5 shows residual densities after refinement *E* [excluding the high-order reflections with $(\sin\theta)/\lambda \geq 1{\cdot}0$ Å^{-1}]. All the positive peaks on the threefold axes diminished and the characteristic features of the *d*-electron asphericity largely deteriorated. These results indicate that the high-order reflection data should necessarily be included in the refinement to avoid unrealistic results. Another criterion is the temperature dependence of the defor-

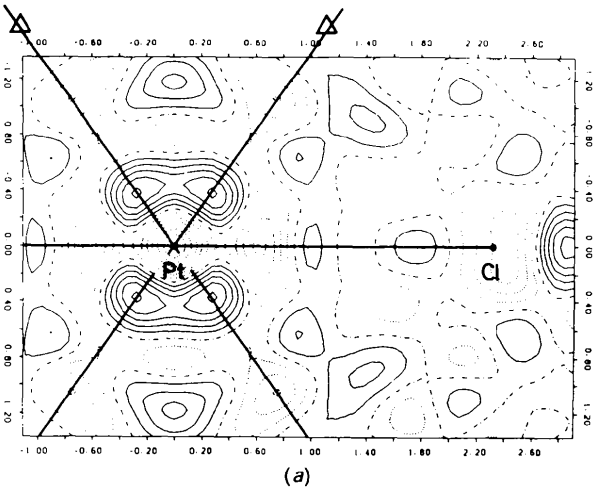

(*a*)

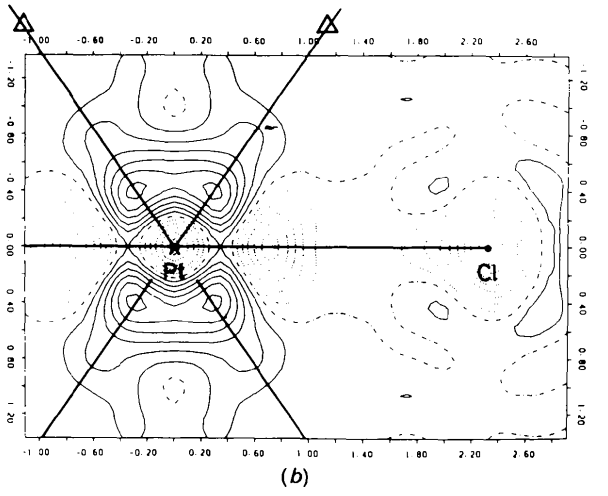

(*b*)

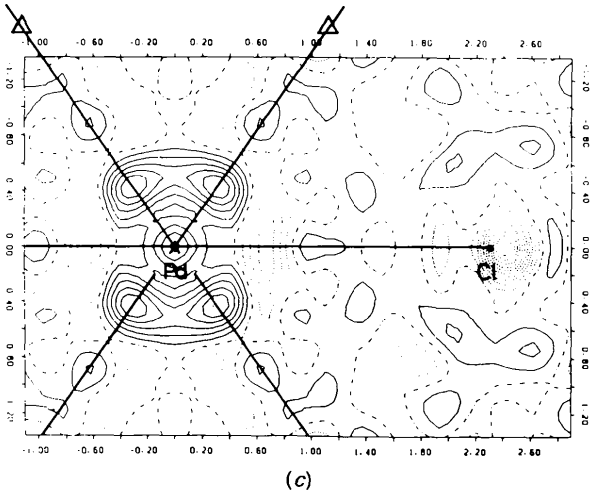

(*c*)

Fig. 4. Residual densities on the (110) plane after refinement *D*. (*a*) For $K_2[PtCl_6]$ (Ag $K\alpha$ data), (*b*) for $K_2[PtCl_6]$ (Mo $K\alpha$ data) and (*c*) for $K_2[PdCl_6]$ (Mo $K\alpha$ data). $[(\sin\theta)/\lambda]_{max} = 1{\cdot}0$ Å^{-1}, contour intervals at 0·2 e Å^{-3}.

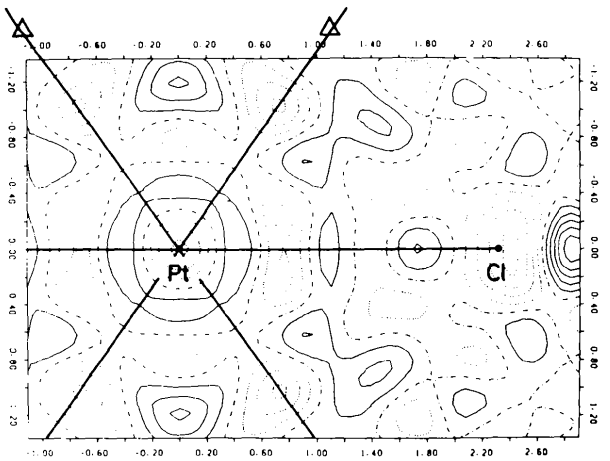

(*a*)

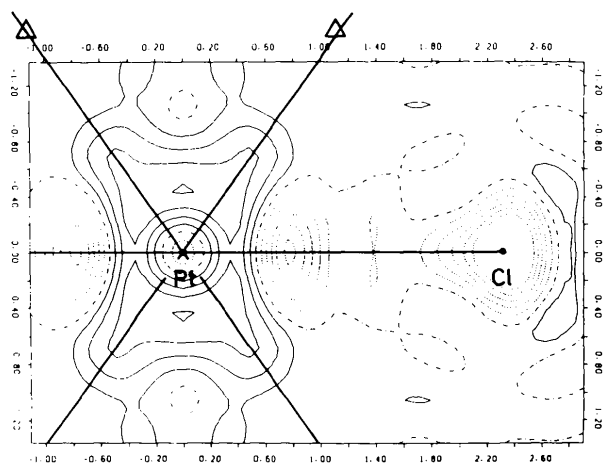

(*b*)

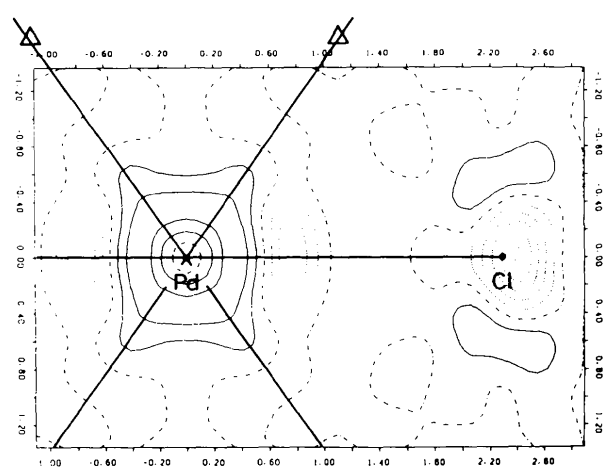

(*c*)

Fig. 5. Residual densities on the (110) plane after refinement *E*. (*a*) For $K_2[PtCl_6]$ (Ag $K\alpha$ data), (*b*) for $K_2[PtCl_6]$ (Mo $K\alpha$ data) and (*c*) for $K_2[PdCl_6]$ (Mo $K\alpha$ data). $[(\sin\theta)/\lambda]_{max} = 1{\cdot}0$ Å^{-1}, contour intervals at 0·2 e Å^{-3}.

mation density. Charge asphericity owing to 5*d* electrons around the Pt atom could indeed be detected more clearly at 120 K than at room temperature (Ohba, Sato, Saito, Ohshima & Harada, 1983; Ohba & Saito, 1984). In conclusion, the present study confirmed that even the 5*d* electrons can be investigated by the X-ray diffraction method.

A part of the present work was supported by a Grant-in-Aid for Scientific Research No. 01790571 from the Ministry of Education, Science and Culture, to which the authors' thanks are due.

References

ADACHI, H., TSUKADA, M. & SATOKO, C. (1978). *J. Phys. Soc. Jpn*, **45**, 875–883.

BECKER, P. J. & COPPENS, P. (1975). *Acta Cryst.* A**31**, 417–425.

BOND, W. L. (1951). *Rev. Sci. Instrum.* **22**, 344–345.

BROWN, T. L., MCDUGLE, W. G. JR & KENT, L. G. (1970). *J. Am. Chem. Soc.* **92**, 3645–3653.

CHATTERJEE, A., MASLEN, E. N. & WATSON, K. J. (1989). *Acta Cryst.* B**44**, 386–395.

CLEMENTI, E. & RAIMONDI, D. L. (1963). *J. Chem. Phys.* **38**, 2686–2689.

COPPENS, P., GURU ROW, T. N., LEUNG, P., STEVENS, E. D., BECKER, P. J. & YANG, Y. W. (1979). *Acta Cryst.* A**35**, 63–72.

EYRING, H., WALTER, J. & KIMBALL, G. E. (1944). *Quantum Chemistry*, pp. 161–163. New York: John Wiley.

FORKESSON, B. & LARSSON, R. (1976). *Chem. Scr.* **10**, 105–109.

HANSEN, N. K. & COPPENS, P. (1978). *Acta Cryst.* A**34**, 909–921.

HOLLADAY, A., LEUNG, P. & COPPENS, P. (1983). *Acta Cryst.* A**39**, 377–387.

IBERS, J. A. & HAMILTON, W. C. (1964). *Acta Cryst.* **17**, 781–782.

IKEDA, R., NAKAMURA, D. & KUBO, M. (1965). *J. Phys. Chem.* **69**, 2101–2107.

International Tables for X-ray Crystallography (1974). Vol. IV. Birmingham: Kynoch Press. (Present distributor Kluwer Academic Publishers, Dordrecht.)

ITO, K., NAKAMURA, D., KURITA, Y., ITO, K. & KUBO, M. (1961). *J. Am. Chem. Soc.* **83**, 4526–4528.

ITO, K., NAKAMURA, D., KURITA, Y., ITO, K. & KUBO, M. (1963). *Inorg. Chem.* **2**, 690–693.

JENNINGS, L. D. (1984). *Acta Cryst.* A**40**, 12–16.

LARSSON, R. & FORKESSON, B. (1977). *Chem. Scr.* **11**, 5–7.

MALLINSON, P. R., KORITSANSZKY, T., ELKAIM, E., LI, N. & COPPENS, P. (1988). *Acta Cryst.* A**44**, 336–342.

MANN, J. B. (1967). *Atomic Structure Calculation* I. Report LA-3690. Los Alamos Scientific Laboratory, Univ. of California, USA.

MARRAM, E. P., MCNIFF, E. J. & RAGLE, J. L. (1963). *J. Phys. Chem.* **67**, 1719.

NAKAMURA, D., KURITA, Y., ITO, K. & KUBO, M. (1960). *J. Am. Chem. Soc.* **82**, 5783–5787.

OHBA, S. & SAITO, Y. (1984). *Acta Cryst.* C**40**, 1639–1641.

OHBA, S., SAITO, Y. & WAKOH, S. (1982). *Acta Cryst.* A**38**, 103–108.

OHBA, S., SATO, S., SAITO, Y., OHSHIMA, K. & HARADA, J. (1983). *Acta Cryst.* B**39**, 49–53.

OHBA, S., TORIUMI, K., SATO, S. & SAITO, Y. (1978). *Acta Cryst.* B**34**, 3535–3542.

STEVENS, E. D. & COPPENS, P. (1976). *Acta Cryst.* A**32**, 915–917.

TAKAZAWA, H., OHBA, S. & SAITO, Y. (1988). *Acta Cryst.* B**44**, 580–585.

TANAKA, K. & MARUMO, F. (1983). *Acta Cryst.* A**39**, 631–641.

WILLIS, B. T. M. (1969). *Acta Cryst.* A**25**, 277–300.